arXiv:cond-mat/0309538v2 [cond-mat.str-el] 28 Oct 2003

Orbital Wave and its Observation in Orbital Ordered Titanates and Vanadates

Sumio Ishihara
Department of Physics, Tohoku University, Sendai 980-8578, Japan

(February 6, 2008)

We present a theory of the collective orbital excitation termed orbital wave in perovskite titanates and vanadates with the triply degenerate t_{2g} orbitals. The dispersion relations of the orbital waves for the orbital ordered LaVO$_3$, YVO$_3$ and YTiO$_3$ are examined in the effective spin-orbital coupled Hamiltonians associated with the Jahn-Teller type couplings. We propose possible scattering processes for the Raman and inelastic neutron scatterings from the orbital wave and calculate the scattering spectra for titanates and vanadates. It is found that both the excitation spectra and the observation methods of the orbital wave are distinct qualitatively from those for the e_g orbital ordered systems.

PACS numbers: 75.10.-b, 75.30.Et, 78.70.-g, 78.70.Nx

I. INTRODCUTION

When degenerate electron orbitals are partially filled in correlated electron systems, this is recognized to be an internal degree of freedom belonging to an electron as well as spin and charge. This orbital degree of freedom has recently attracted much attention especially in transition-metal (TM) oxides.[1,2] In particular, the orbital ordering (OO) and fluctuation play a key role in anisotropic electric, magnetic and optical properties in correlated oxides.

The collective orbital excitation in the orbital ordered state is known to be orbital wave (OW), in analogous to the spin wave in magnetically ordered state, and its quantized object is termed orbiton. The theoretical study of OW has started in the idealized spin-orbital coupled model where the continuous symmetry exists in the orbital space,[3] and progressed in the anisotropic orbital model.[4] A realistic calculation has been done in LaMnO$_3$ with the doubly degenerate e_g orbitals.[5] Recently new peak structures observed in the Raman spectra in LaMnO$_3$ are interpreted as scatterings from OW.[6] Although there are some debates about origin of the newly found peaks, OW or multiphonons,[7,8] the energy and polarization dependences of the observed Raman spectra show a good agreement with the calculation based on the OW interpretation.

The perovskite titanates RTiO$_3$ and vanadates RVO$_3$ (R: rare-earth ion) with the triply degenerate t_{2g} orbitals are another class of materials where OW is expected. One of the well known orbital ordered materials is YTiO$_3$ where the nominal valence of the titanium ion is 3+ and one electron occupies the triply degenerate t_{2g} orbitals. The orbital ordered state associated with the Jahn-Teller (JT) type lattice distortion has been confirmed by the resonant x-ray scatterings, NMR and the polarized neutron scattering experiments and so on.[9–12] These results almost coincide with each other: there are four different orbitals in a unit cell where the wave functions are given as $\frac{1}{\sqrt{2}}(d_{xy}+d_{yz})$, $\frac{1}{\sqrt{2}}(d_{xy}-d_{yz})$, $\frac{1}{\sqrt{2}}(d_{xy}+d_{zx})$ and $\frac{1}{\sqrt{2}}(d_{xy}-d_{zx})$.[13] This type of OO, termed the $(d_{y(x+z)}/d_{y(x-z)}/d_{x(y+z)}/d_{x(y-z)})$-type from now on, is also supported by previous calculations.[14–16] Although an exotic orbital state is proposed recently by taking into account the quantum fluctuation,[17,18] the predicted orbital state being incompatible with the crystal lattice symmetry is different from the above type of OO.

A series of RVO$_3$ is systematically examined in the recent studies.[14,15,19–30] Two electron occupy the triply degenerate orbitals in a V^{3+} ions. A sequential phase transition is found in YVO$_3$;[19–21] the G-type OO (O-G) occurs at T_{OO1}=200K and the C-type antiferromagnetic (AFM) ordering (S-C) appears at T_{N1}=115K. With further decreasing temperature, another orbital and magnetic transitions appear at $T_{N2}=T_{OO2}$=77K where the C-type OO associated with the G-type AFM order (the (S-G/O-C) order) is realized. On the other hand, in LaVO$_3$, the C-type AFM ordering occurs at T$_N$(=143K) and, at slightly below this temperature, the G-type OO (the (S-C/O-G) order) appears.[20–22] Types of OO in vanadates are determined that the d_{xy} orbital is occupied at all the vanadium sites and the d_{yz} and d_{zx} orbitals are alternately ordered in the xy plane (the C-type OO), and in all direction (the G-type OO).[24,25] These kinds of OO are termed the pure OO states, and the OO such as realized in YTiO$_3$ is termed the mixed OO from now on. It is suggested that the experimentally observed type of OO in vanadates associated with the JT type distortion explains the several optical and magnetic properties.[28,29]

Here, we present a theory of OW in titanates and vanadates where the orbital ordered states are confirmed experimentally well. The dispersion relations of OW are examined in the (S-C/O-G)- and (S-G/O-C)-phases for LaVO$_3$, YVO$_3$ (the low temperature phase), respectively, and the $(d_{y(x+z)}/d_{y(x-z)}/d_{x(y+z)}/d_{x(y-z)})$-type OO for YTiO$_3$. The calculations are based on the effective spin-orbital coupled Hamiltonians associated with the JT type electron-lattice coupling. We propose possible scattering processes for the Raman and inelastic neutron scatterings from OW and calculate the spectra. It is found that the excitation spectra and the observation methods of OW are distinct qualitatively from those for the e_g orbital ordered systems such as manganites.

In Sec. II, the model Hamiltonian for titanates and vanadates with the triply degenerate t_{2g} orbitals are introduced. In Sec. III, the dispersion relations of OW for LaVO$_3$, YVO$_3$ and YTiO$_3$ are examined. The scattering spectra for the Raman and inelastic neutron scatterings from OW are shown in Sec. IV. Section V is devoted to summary and discussion.

II. MODEL HAMILTONIAN

The collective orbital excitations in the orbital ordered state are studied in the spin-orbital model derived from the generalized Hubbard Hamiltonian with the triply degenerate t_{2g} orbitals:

$$\begin{aligned}\mathcal{H} = {} & \varepsilon_d \sum_{i,\sigma,\gamma} d^\dagger_{i\gamma\sigma} d_{i\gamma\sigma} + \mathcal{H}_{el-el} \\ & + \sum_{\langle ij\rangle,\gamma,\gamma',\sigma} \left(t^{\gamma\gamma'}_{ij} d^\dagger_{i\gamma\sigma} d_{j\gamma'\sigma} + H.c. \right),\end{aligned} \tag{1}$$

with the electron-electron interaction term

$$\begin{aligned}\mathcal{H}_{el-el} = {} & U \sum_{i,\gamma} n_{i\gamma\uparrow} n_{i\gamma\downarrow} + U' \sum_{i,\gamma>\gamma'} n_{i\gamma} n_{i\gamma'} \\ & + I \sum_{i,\gamma>\gamma',\sigma,\sigma'} d^\dagger_{i\gamma\sigma} d^\dagger_{i\gamma'\sigma'} d_{i\gamma\sigma'} d_{i\gamma'\sigma} \\ & + J \sum_{i,\gamma\neq\gamma'} d^\dagger_{i\gamma\uparrow} d^\dagger_{i\gamma\downarrow} d_{i\gamma'\downarrow} d_{i\gamma'\uparrow}.\end{aligned} \tag{2}$$

$d_{i\gamma\sigma}$ is the annihilation operator for the t_{2g} electron at site i with spin $\sigma = (\uparrow, \downarrow)$ and orbital $\gamma = (yz, zx, xy)$. The number operators are defined by $n_{i\gamma\sigma} = d^\dagger_{i\gamma\sigma} d_{i\gamma\sigma}$ and $n_{i\gamma} = \sum_\sigma n_{i\gamma\sigma}$. U and U' are the intra- and inter-orbital Coulomb interactions, respectively, I is the exchange interaction, and J is the pair-hopping interaction. $t^{\gamma\gamma'}_{ij}$ in Eq. (1) is the electron transfer integral between site i with orbital γ and nearest neighboring (NN) site j with γ'. In the ideal perovskite structure, the hopping integral is simplified as $t^{\gamma\gamma'}_{ij} = t_0 \delta_{\gamma\gamma'} (\delta_{\gamma=(lh)} + \delta_{\gamma=(kl)})$ where l indicates a direction of a bond connecting sites i and j, and $(h,k,l) = (x,y,z)$, (y,z,x), (z,x,y). The electron hopping occurs through the O $2p$ orbitals in between the NN TM sites.

We derive the effective Hamiltonian for titanates where the nominal electron configuration of the TM ion is d^1. This Hamiltonian is defined in the Hilbert space where the electron number per site is restricted to be one or less due to the strong on-site Coulomb interactions. The Hamiltonian is classified by the intermediate states of the perturbational processes as derived in Ref. 13;

$$\mathcal{H}_{\rm Ti} = \mathcal{H}_{T_1} + \mathcal{H}_{T_2} + \mathcal{H}_E + \mathcal{H}_{A_1}, \tag{3}$$

with

$$\mathcal{H}_{T_1} = -J_{T_1} \sum_{\langle ij\rangle} \left(\frac{3}{4} + \vec{S}_i \cdot \vec{S}_j \right) \left(A^l_- + B^l - C^l_+ \right), \tag{4}$$

$$\mathcal{H}_{T_2} = -J_{T_2} \sum_{\langle ij\rangle} \left(\frac{1}{4} - \vec{S}_i \cdot \vec{S}_j \right) \left(A^l_- + B^l + C^l_+ \right), \tag{5}$$

$$\mathcal{H}_E = -J_E \sum_{\langle ij\rangle} \left(\frac{1}{4} - \vec{S}_i \cdot \vec{S}_j \right) \frac{2}{3} \left(2A^l_+ - C^l_- \right), \tag{6}$$

$$\mathcal{H}_{A_1} = -J_{A_1} \sum_{\langle ij\rangle} \left(\frac{1}{4} - \vec{S}_i \cdot \vec{S}_j \right) \frac{2}{3} \left(A^l_+ + C^l_- \right). \tag{7}$$

The superexchange interactions are given by $J_\Gamma = t_0^2/E^{(2)}_\Gamma$ ($\Gamma = T_1,\ T_2,\ E, A_1$) where $E^{(2)}_\Gamma$'s are the energies of the intermediate states: $E^{(2)}_{T_1} = U' - I$, $E^{(2)}_E = U - I$, $E^{(2)}_{T_2} = U' + I$ and $E^{(2)}_{A_1} = U + 2I$ where the relations $U = U' + 2I$ and $I = J$ are used. J_{T_1} is the largest among them. The spin degree of freedom is described by the operator $\vec{S}_i = \frac{1}{2} \sum_{\gamma s s'} d^\dagger_{i\gamma s} \vec{\sigma}_{ss'} d_{i\gamma s'}$ with the Pauli matrices $\vec{\sigma}$. The orbital degree of freedom is represented by the eight orbital operators $O_{i\Gamma\gamma}$ classified by the irreducible representations of the O$_{\rm h}$ group as $(\Gamma\gamma) = (Eu)$, (Ev), (T_2x), (T_2y), (T_2z), (T_1x), (T_1y), (T_1z). These operators are defined by the generators of the SU(3) Lie algebra, i.e. the 3×3 Gell-Mann matrices λ_m ($l = m \sim 8$) as[31]

$$O_{i\Gamma\gamma} = \frac{-1}{\sqrt{2}} \sum_{\sigma,\alpha,\beta} d^\dagger_{i\alpha\sigma} \lambda_{m\alpha\beta} d_{i\beta\sigma}, \tag{8}$$

where $(\Gamma\gamma, m) = (Eu, 8)$, $(Ev, 3)$ $(T_2x, 6)$, $(T_2y, 4)$, $(T_2z, 1)$, $(T_1x, 7)$, $(T_1y, 5)$, $(T_1z, 2)$. The operators $O_{iE\gamma}$ and $O_{iT_2\gamma}$ represent the diagonal and off-diagonal components of the electric quadrupole moments, respectively, and $O_{iT_1\gamma}$ does the magnetic dipole ones, i.e. the orbital angular momentum. By utilizing the above orbital operators, the orbital parts of the Hamiltonian in Eqs. (4)-(7) are given as

$$A^l_\pm = W^l_i W^l_j \pm O^l_{iEv} O^l_{jEv}, \tag{9}$$

$$B^l = V^l_i W^l_j + W^l_i V^l_j, \tag{10}$$

$$C^l_\pm = 2 \left(O_{iT_2l} O_{jT_2l} \pm O_{iT_1l} O_{jT_1l} \right), \tag{11}$$

with

$$W^l_i = \frac{2}{3} - \sqrt{\frac{2}{3}} O^l_{iEu}, \tag{12}$$

$$V^l_i = \frac{1}{3} + \sqrt{\frac{2}{3}} O^l_{iEu}. \tag{13}$$

O^l_{iEu} and O^l_{iEv} are defined by

$$\begin{pmatrix} O^l_{iEu} \\ O^l_{iEv} \end{pmatrix} = \begin{pmatrix} \cos\frac{2\pi}{3}m_l & \sin\frac{2\pi}{3}m_l \\ -\sin\frac{2\pi}{3}m_l & \cos\frac{2\pi}{3}m_l \end{pmatrix} \begin{pmatrix} O_{iEu} \\ O_{iEv} \end{pmatrix}, \quad (14)$$

with $m_l = (1, 2, 3)$ for a direction of the bond $l = (x, y, z)$. In analogy with the spin Hamiltonian, $A^l_\pm$ and B^l correspond to the $S_{iz}S_{jz}$ term, and C^l_+ and C^l_- to the $S_{i+}S_{j-} + S_{i-}S_{j+}$ and $S_{i+}S_{j+} + S_{i-}S_{j-}$ terms respectively. The latter term originates form the pair hopping processes which break the conservation of the total electron number at each orbital, e.g. $\sum_i \langle n_{ixy} \rangle$.

The effective Hamiltonian for vanadates, where the nominal electron configuration is d^2, is derived in a similar way from Eq. (1). The d^2 state is assumed to be the lowest ${}^3T_1$ state due to the Hund rule. The explicit form is given by

$$\mathcal{H}_\mathrm{V} = \mathcal{H}_{A_1} + \mathcal{H}_E + \mathcal{H}_{T_1} + \mathcal{H}_{T_2}, \quad (15)$$

with

$$\mathcal{H}_{A_1} = -J_{A_1} \sum_{\langle ij \rangle} \frac{1}{6} \left(2 + \vec{S}_i \cdot \vec{S}_j \right) \times \left(-A^l_+ + A^l_- + B^l - 2C^l_+ \right), \quad (16)$$

$$\mathcal{H}_E = -J_E \sum_{\langle ij \rangle} \frac{1}{6} \left(1 - \vec{S}_i \cdot \vec{S}_j \right) \times \left(-A^l_+ + A^l_- + B^l + C^l_+ \right), \quad (17)$$

$$\mathcal{H}_{T_1} = -J_{T_1} \sum_{\langle ij \rangle} \frac{1}{4} \left(1 - \vec{S}_i \cdot \vec{S}_j \right) \left(A^l_+ - C^l_- \right), \quad (18)$$

$$\mathcal{H}_{T_2} = -J_{T_2} \sum_{\langle ij \rangle} \frac{1}{4} \left(1 - \vec{S}_i \cdot \vec{S}_j \right) \left(A^l + C^l_- \right). \quad (19)$$

We introduce the spin operator $\vec{S}_i$ with a magnitude $S = 1$, and the exchange parameters defined by $J_\Gamma = t_0^2/\Delta E_\Gamma$ where $\Delta E_\Gamma = E^{(3)}_\Gamma - E^{(2)}_{T_1}$ with $\Delta E_{A_1} = U' - I$, $\Delta E_E = \Delta E_{T_1} = U' + 2I$ and $\Delta E_{T_2} = U' + 4I$. It is noted that a similarity between $\mathcal{H}_\mathrm{Ti}$ and $\mathcal{H}_\mathrm{V}$ is attributed to the fact that, with respect to the orbital degree of freedom, the high spin ${}^3T_1$ state for the d^2 configuration in the hole picture is equivalent to the d^1 state in the electron picture. Similar types of the spin-orbital coupled Hamiltonian in the triply degenerate t_{2g} orbitals are also derived by several authors for the d^1 and d^2 systems[16,18,27,30,32,33]

In addition to the electronic Hamiltonian, the electron-lattice interactions are introduced. In the t_{2g} orbital systems, there are two kinds of the JT type interactions;

$$\mathcal{H}_{JT} = g_E \sum_{i,\gamma=(u,v)} Q_{iE\gamma} O_{iE\gamma} + g_{T_2} \sum_{i,\gamma=(x,y,z)} Q_{iT_2\gamma} O_{iT_2\gamma}, \quad (20)$$

where g_E and g_{T_2} are the coupling constants and $Q_{iE\gamma}$ and $Q_{iT_2\gamma}$ are the normal modes in an O_6 octahedron with symmetries E_g and T_{2g}, respectively. $Q_{E\gamma}$ directly modifies the TM-O bond lengths and $Q_{T_2\gamma}$ modifies the O-TM-O bond angles.

Energy parameter values have been numerically evaluated by several authors. The effective exchange parameters J^S in the Heisenberg model are obtain from the spin-wave dispersion relations as J^S_z=5.5meV (z axis) and J^S_{xy}=5.8meV (xy plane) in the (S-G/O-C) phase in $\mathrm{YVO_3}$, $J^S_z = 2.2 - 4$meV, J^S_{xy} =2.6meV in the (S-C/O-G) phase in $\mathrm{YVO_3}$ (Ref. 26), and $J^S_z = J^S_{xy}$=3meV in $\mathrm{YTiO_3}$ (Ref. 17). The effective exchange parameters for the orbital operators in $\mathrm{LaVO_3}$ are also estimated as $J^O_z \equiv 4t_0^2/(U' - I)$=33meV and J^O_{xy}=2meV (Ref. 28). The JT stabilization energy is obtained from the LDA+U method[28] as E_{JT}=27meV which is comparable or larger than the exchange interactions. The relativistic spin-orbit interaction which is not taken into account in the present model is about 0.4meV being much smaller than both the exchange and JT energies.[15] This is consistent with the experimental results in the magnetic x-ray scattering in $\mathrm{YTiO_3}$; the angular momentum separately estimated from the spin momentum is found to be negligible small.[34] Thus, the Hamiltonian $\mathcal{H}_{\mathrm{Ti(V)}} + \mathcal{H}_{JT}$ introduced above is the minimal model for examination of OW.

Here we mention the implications of the theoretical model for the observed spin/orbital orders. As we have shown in Ref. 13, in the mean field theory, the large orbital degeneracy remains in the ferromagnetic (FM) ground state in $\mathcal{H}_\mathrm{Ti}$. A small perturbation, such as the Jahn-Teller type distortion, the relativistic spin-orbit coupling, the $\mathrm{GdFeO_3}$-type lattice distortion, lifts the degeneracy. We suppose that the Jahn-Teller type distortion with the T_{2g} symmetry, $g_{T_2}Q_{iT_2}$ in Eq. (20), plays a key role to stabilize the observed mixed orbital order. The (S-C/O-G) order for $\mathrm{LaVO_3}$ is reproduced by $\mathcal{H}_\mathrm{V}$. The FM (AFM) order along the c axis (in the ab plane) is attributed to the alternate (uniform) alignment of the d_{yz} and d_{zx} orbitals (the d_{xy} orbital) along the c axis (in the ab plane). The (S-G/O-C) order for the $\mathrm{YVO_3}$ is obtained by $\mathcal{H}_\mathrm{V}$ and the Jahn-Teller type interaction with the E_g symmetry. The AFM spin order and the uniform alignment of the $d_{yz}(d_{zx})$ orbital along the c axis is stabilized cooperatively, as discussed in the next section.

III. ORBITAL WAVE

The dispersion relations of OW in the orbital ordered states are obtained by utilizing the Holstein-Primakoff transformation for the generators in the SU(3) algebra.[35,36] For example, at a site where the d_{xy} orbital is occupied, there are two excitation modes; an excitation between the d_{xy} and d_{yz} orbitals denoted by a boson operator y ($y^\dagger$), and that between d_{xy} and d_{zx} denoted by x ($x^\dagger$). The orbital operators $O_{i\Gamma\gamma}$ are transformed into

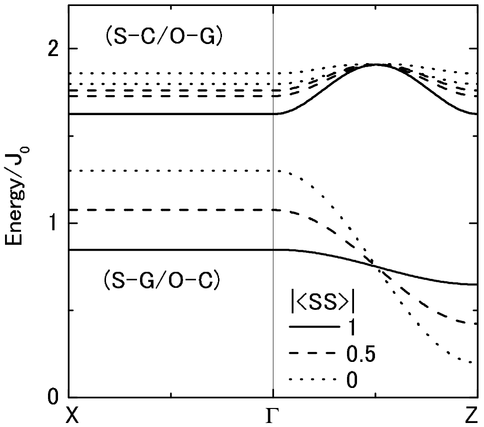

FIG. 1. Dispersion relations of OW in the (S-C/O-G) and (S-G/O-C)-phases for LaVO$_3$ and YVO$_3$ (the low temperature phase), respectively. The absolute values of the spin correlation function between NN sites $|\langle \vec{S}_i \cdot \vec{S}_{i+\delta}\rangle|$ are 1 (bold lines), 0.5 (broken lines) and 0 (dotted lines). The parameter values are chosen to be I/U'=0.125. $g_E Q_E/J_0$=0.8 and $g_{T_2}Q_{T_2}$=0. The dispersion curves in the (S-G/O-C) phase and the curve in the (S-C/O-G) phase with $|\langle \vec{S}_i \cdot \vec{S}_{i+\delta}\rangle| = 1$ are doubly degenerate.

these boson operators as

$$
\begin{aligned}
O_{iEu} &= \sqrt{\frac{2}{3}} - \sqrt{\frac{3}{2}}\left(n_{ix}+n_{iy}\right), \\
O_{iEv} &= \frac{1}{\sqrt{2}}\left(n_{iy}-n_{ix}\right), \\
O_{iT_\alpha z} &= \begin{pmatrix} -i \\ 1 \end{pmatrix}_\alpha \left(y_i^\dagger x_i \pm x_i^\dagger y_i\right), \\
O_{iT_\alpha y} &= \begin{pmatrix} i \\ 1 \end{pmatrix}_\alpha \left(\sqrt{1-N_i}\,y_i \pm y_i^\dagger \sqrt{1-N_i}\right), \\
O_{iT_\alpha x} &= \begin{pmatrix} -i \\ 1 \end{pmatrix}_\alpha \left(x_i^\dagger \sqrt{1-N_i} \pm \sqrt{1-N_i}\,x_i\right), \qquad (21)
\end{aligned}
$$

with $\alpha = (1,2)$. The plus and minus signs in $O_{iT_\alpha x}$, $O_{iT_\alpha y}$ and $O_{iT_\alpha z}$ are for the $\alpha=1$ and $\alpha=2$ cases, respectively. We define $N_i = n_{ix}+n_{iy}$ with $n_{ix} = x_i^\dagger x_i$ and $n_{iy} = y_i^\dagger y_i$. In the linear spin wave approximation, $\sqrt{1-N_i}$ is replaced by 1. We have cheked that the Green's function method for the operators $O_{i\Gamma\gamma}$, i.e. $G_{\Gamma\gamma\Gamma'\gamma'}(t-t', \vec{r}_i - \vec{r}_{i'}) = -i\theta(t-t')\langle[O_{i\Gamma\gamma}(t), O_{i'\Gamma'\gamma'}(t')]\rangle$, with the decoupling approximation, reproduces the calculated results for OW with the boson method introduced above.

In Fig. 1, we present the dispersion relations of OW in the (S-C/O-G) and (S-G/O-C) phases for LaVO$_3$ and YVO$_3$ (the low temperature phase), respectively. The parameter values are chosen to be $I/U' \equiv R$=0.125, $g_E Q_E/J_0$=0.8 and $g_{T_2}Q_{T_2}$=0. The energy parameters are normalized by $J_0 = 4t_0^2/(U'-I)$ which is estimated to be about 33meV for LaVO$_3$ (Ref. 28) and is supposed to be smaller in YTiO$_3$ due to the larger GdFeO$_3$-type lattice distortion. The ratios of the exchange parameters are represented by the parameter R as $J_{T_2}/J_{T_1} = J_E/J_{T_1} = (1-R)/(1+2R)$ and $J_{A_1}/J_{T_1} = (1-R)/(1+4R)$. Both the (S-C/O-G)- and (S-G/O-C)-phases, there are four modes of OW attributed to the two different orbital occupied sites in a unit cell; there are the excitations y_A ($d_{xy} \to d_{yz}$) and z_A ($d_{zx} \to d_{yz}$) at site A where the d_{xy} and d_{zx} orbitals are occupied, and the excitations x_B ($d_{xy} \to d_{zx}$) and z_B ($d_{yz} \to d_{zx}$) at site B where the d_{xy} and d_{yz} orbitals are occupied. Two of the four, i.e. y_A and x_B, are the local modes within the linear spin wave theory and do not show dispersions. This character does not depend on the spin arrangements. These local modes originate from the facts that (1) the excited d_{xy} hole does not hop along the z axis due to the orbital symmetry, and (2) a coherent motion of the excited d_{xy} hole in the xy plane are impossible, since this motion is associated with increasing the number of the wrong orbital arrangements. The latter implies that the orbital exchange processes do not recover the wrong orbital arrangements, and the triply degenerate orbital model is qualitatively different from the Heisenberg model with $S=1$. The remaining modes, z_A and z_B, are dispersive along the z direction. The dispersion relation of OW in the (S-C/O-G) phase is explicitly obtained as $E(\vec{k}) = \frac{8}{6}J_{A_1}\sqrt{(K_2^x + K_2^z)^2 - (\frac{3}{2}K_1^z \cos ak_z)^2}$ where we assume $I=0$ and $g_E Q_E = g_{T_2}Q_{T_2} = 0$. We introduce $K_2^{x(z)} = 2 + \langle \vec{S}_i \cdot \vec{S}_{i+\delta_x(\delta_z)}\rangle$ and $K_1^{x(z)} = 1 - \langle \vec{S}_i \cdot \vec{S}_{i+\delta_x(\delta_z)}\rangle$. This energy has its minimum at $k_z = 0$ and the energy gap is attributed to the anisotropy in the orbital space, i.e. a lack of the SU(3) symmetry, in the orbital part of the Hamiltonian. In comparison with the OW in the (S-C/O-G) phase, the OW in the (S-G/O-C) phase is barely stable; with decreasing the spin correlation which corresponds to increasing temperature toward T_N, a remarkable softening around $\vec{k} = (0,0,\pi)$ occurs. In the case where $I=0$ and $g_{T_2}Q_{T_2} = 0$, the dispersion relation is given as $E(\vec{k}) = \frac{2}{3}J_{A_1}(2K_2^z - K_1^z)\cos ak_z + \sqrt{\frac{3}{2}}g_E Q_E$ which has its minimum value at $k_z = \pi$, and the energy gap is attributed to the JT type interaction. This result suggests an instability of the (S-G/O-C) phase to the (S-C/O-G) one with increasing temperature. This is consistent with the experimental fact that in RVO$_3$ the O-C phase appears associated with the S-G order, and is changed into the (S-C/O-G) phase at 77K in YVO$_3$.[21]

In Fig. 2, we present the dispersion relations of OW in the $(d_{y(x+z)}/d_{y(x-z)}/d_{x(y+z)}/d_{x(y-z)})$-type OO for YTiO$_3$. The FM and paramagnetic spin orders are assumed, and the exchange parameter is taken to be $R \equiv I/U' = 0.125$. The JT type interaction parameters are chosen to be $g_E Q_E/J_0 = g_{T_2}Q_{T_2}/J_0 = 1.2$, where $g_E Q_E$ is larger than that in vanadates and $g_{T_2}Q_{T_2}$ is introduced. This is based on a consideration that, in comparison with vanadates, J_0 is supposed to be smaller due to the large GeFeO$_3$-type lattice distortion, and Q_{T_2} is found to be

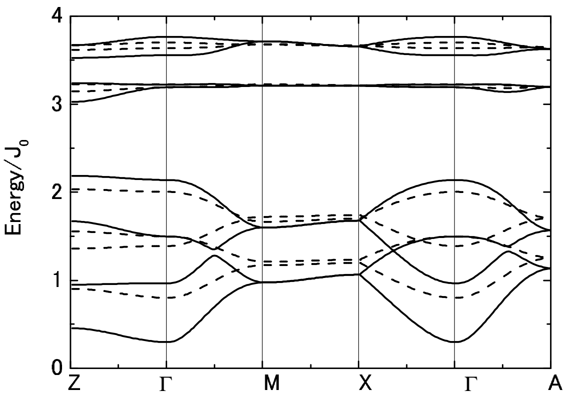

FIG. 2. Dispersion relations of OW in the $(d_{y(x+z)}/d_{y(x-z)}/d_{x(y+z)}/d_{x(y-z)})$-type OO for YTiO$_3$. The bold and broken lines are for the FM and paramagnetic states, respectively. The parameter values are chosen to be I/U'=0.125, $g_E Q_E/J_0$=$g_{T_2}Q_{T_2}/J_0$=1.2. The Brillouin zone for the tetragonal symmetry is adopted.

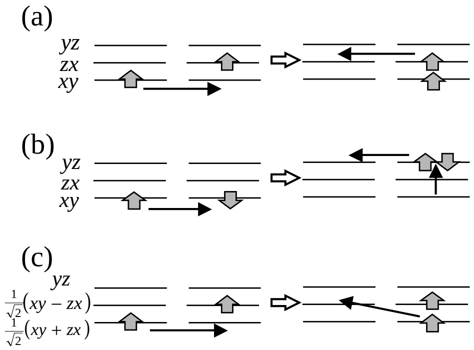

FIG. 3. Scattering processes in the Raman scattering. (a) and (b) The two-orbiton scattering processes in the pure OO states. (c) The one-orbiton scattering processes in the mixed OO state.

larger in the crystal structure of YTiO$_3$.[12,22,23] In contrast to the case of vanadates, all the eights modes, attributed to the four different orbitals in a unit cell, are dispersive along all the directions in the Brillouin zone. This originates from the OO states with the mixed orbitals where the excitations propagate along the three directions. The OW dispersions are classified into the two groups: for example, in the $\frac{1}{\sqrt{2}}(d_{xy}+d_{yz})$ orbital occupied site, the higher energy bands with smaller band widths are mainly attributed to the excitations to the d_{zx} orbital, and the lower energy ones with a larger width are attributed to the excitations to the $\frac{1}{\sqrt{2}}(d_{xy}-d_{yz})$ orbital.

IV. OBSERVATION OF ORBITAL WAVE

A. raman scattering

As introduced in Sec. I, in orbital ordered LaMnO$_3$, the new peak structures in the Raman spectra were explained successfully as the scattering from OW.[6] Here we consider the Raman scattering as a possible probe to detect the OW in titanates and vanadates with the triply degenerate t_{2g} orbitals. It is considered the inter-site scattering processes where OW's are excited through the electronic exchange processes between the NN TM sites.[37,38] This is attributed to the fact that the lowest electronic excitations in titanates and vanadates occur across the Mott-Hubbard gap, unlike the manganites where the electronic excitations across the charge-transfer gap dominate the excitation of OW. Depending on the types of OO, there are the following two scattering processes: (i) The two-orbiton scattering: Consider a pair of the NN TM sites where the occupied orbitals are different and the pure orbitals (Fig. 3), such as the OO in vanadates. Through the second order processes of the interaction between photons and electrons, electrons at the two sites are exchanged and, at the final state, the occupied orbitals are changed at both the sites. This is the analogous to the two magnon Raman scattering in the antiferromagnets. Another two-orbiton process occurs in a pair of the NN TM site where the same kind of orbitals are occupied. In the intermediate state of the scattering process, where two electrons occupy the same orbital at a site, the occupied orbital is changed due to the pair-hopping interaction. At the final state, the two orbitons are created. (ii) The one-orbiton scattering: When the electrons occupy the so-called mixed orbital such as that in YTiO$_3$, the electron hops from one orbital (γ) to the different orbital (γ') in its NN TM site. When this electron comes back to the orbital γ' in the initial site, one orbiton is excited.

There are alternate two scattering processes from OW where one orbton is created at a TM site. (i) An electron is excited from a orbital γ to γ' at the same site associated with a creation of odd-parity phonons. Then, these phonons are annihilated by emitting a photon. Such kinds of the Frank-Condon processes have been considered for the orbiton+phonon excitation in the optical conductivity spectra, and for the multiphonon excitation in the Raman spectra.[39] The total scattering-cross section ratio of this process to the inter-site process is of the order of $10^{-3} \sim 10^{-2}$. (ii) The incident photon excites an electron from the $3d$ γ orbital to one of the $4p$ orbitals at the same site. Then, this electron is relaxed to the $3d$ γ' orbital by emitting a photon. This scattering-cross section ratio to the inter-site process is estimated for titanates and vanadates to be of the order of 10^{-1}.

Here, we calculate the Raman spectra for the inter-site scattering process. It is supposed that this process provides the main contribution for the OW scattering, in particular, in the two-orbiton energy regions. The energy, momentum and polarization of initial (scattered) photon are $\omega_i(\omega_f)$, $\vec{k}_i(\vec{k}_f)$ and $\lambda_i(\lambda_f)$, respectively. The differential scattering cross section from OW is given as

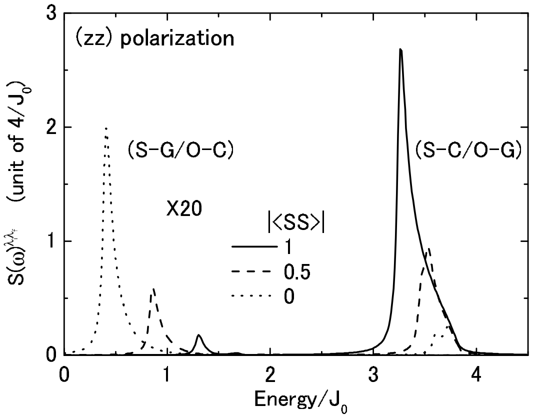

FIG. 4. Raman spectra $S^{\lambda_i\lambda_f}(\omega)$ for the (S-C/O-G)- and (S-G/O-C) phase for LaVO$_3$ and YVO$_3$ (the low temperature phase), respectively. The two-orbiton scattering is considered. The absolute values of the spin correlation function between NN sites $|\langle\vec{S}_i\cdot\vec{S}_{i+\delta}\rangle|$ are 1 (bold lines), 0.5 (broken lines) and 0 (dotted lines). Both the incident and scattered photon polarizations are parallel to the z axis. Other parameter values are the same as those in Fig. 1.

$$\frac{d^2\sigma}{d\Omega dE_f}=\sigma_T\frac{\omega_f}{\omega_i}\left(\frac{ma^2}{\hbar^2}\right)^2\frac{1}{2\pi\hbar}\int dte^{i\hbar(\omega_f-\omega_i)t}\\ \times\sum_{ll'}P_{ll'}S^{ll'}(t), \tag{22}$$

with $\sigma_T=(e^2/mc^2)^2$ and a bond length a. $P_{ll'}$ is the polarization factor given by

$$P_{ll'}=(\vec{e}_{k_i\lambda_i})_l\,(\vec{e}_{k_i\lambda_i})_{l'}\,\left(\vec{e}_{k_f\lambda_f}\right)_l\,\left(\vec{e}_{k_f\lambda_f}\right)_{l'}, \tag{23}$$

and $S^{ll'}(t)$ is the dynamical correlation function defined by

$$S^{ll'}(t)=\langle\mathcal{K}^l(t)\mathcal{K}^{l'}(0)\rangle, \tag{24}$$

with

$$\mathcal{K}^l=\sum_\Gamma\sum_i\sum_{\delta_l}\mathcal{H}_\Gamma(i,i+\delta_l). \tag{25}$$

$\mathcal{H}_\Gamma(i,i+\delta_l)$ is a term of the effective Hamitonian given in Eqs. (3) and (15) concerning with a bond connecting site i and site $i+\delta_l$. Here, $l(=x,y,z)$ indicates a direction of the bond and $\delta_l=\pm\hat{l}$. The index $\Gamma(=T_1,T_2,A_1,E)$ classifies the intermediate states. The exchange interaction $J_\Gamma=t_0^2/\Delta E_\Gamma$ in $\mathcal{H}_\Gamma$ is replaced by $t_0^2/(\Delta E_\Gamma-(\omega_i-\omega_f))$ in $\mathcal{H}_\Gamma(i,i+\delta_l)$. This expression is obtained from the second order processes of the interactions between photons and electronic currents between the NN TM sites.

We introduce the orbiton operators $\widetilde{\psi}(\vec{k})$ with the energies $E(\vec{k})$ which are obtained by diagonalizing the Hamiltonian represented by the Holstein-Primakoff boson operators $\psi(\vec{k})$. This Bogoliubov transformation is given by the matrix $V(\vec{k})$ as

$$\widetilde{\psi}_\alpha(\vec{k})=\sum_\beta\psi_\beta(\vec{k})V_{\beta\alpha}(\vec{k}). \tag{26}$$

$\widetilde{\psi}(\vec{k})$ has $2N$ components in the system where the number of the OW mode is N, and $\widetilde{\psi}_\alpha(\vec{k})$ $(\alpha>N)$ is the creation operator with the condition $\widetilde{\psi}_\alpha(\vec{k})=\widetilde{\psi}_{\alpha-N}(-\vec{k})^\dagger$. For example,

$$\widetilde{\psi}(\vec{k})=\left\{a_1(\vec{k}),\cdots a_N(\vec{k}),a_1^\dagger(-\vec{k}),\cdots a_N^\dagger(-\vec{k})\right\}. \tag{27}$$

By using the oprators, we obtain

$$\mathcal{K}^l=\sum_{\vec{k},\alpha,\beta}\widetilde{\psi}_\alpha(\vec{k})^\dagger h^l_{\alpha\beta}(\vec{k})\widetilde{\psi}_\beta(\vec{k})\\ +\frac{1}{2}\sum_\alpha\left(g^l_\alpha\widetilde{\psi}_\alpha(0)+g^{l*}_\alpha\widetilde{\psi}^\dagger_\alpha(0)\right), \tag{28}$$

where $h^l_{\alpha\beta}(\vec{k})$ and g^l_α are the coefficients. In the pure OO states, the second term vanishes, i.e. the one-orbiton scattering is prohibited. Then the Fourier transform of the dynamical correlation function in the two-orbiton Raman scattering is given by

$$S^{ll'}(\omega)=N\sum_{\vec{k}}\sum_{\alpha=N+1}^{2N}\sum_{\beta=1}^{N}\delta\left\{\omega-E_\alpha(\vec{k})-E_\beta(\vec{k})\right\}\\ \times\left\{h^l_{\alpha\beta}(\vec{k})h^{l'}_{\beta\alpha}(\vec{k})+h^l_{\alpha\beta}(\vec{k})h^{l'}_{\alpha-N\beta+N}(\vec{k})\right\}. \tag{29}$$

We neglect the orbiton-orbiton interaction for simplicity, and $S^{ll'}(\omega)$ is represented by the convolution of the two OW modes. On the other hand, in the one-orbiton scattering, the dynamical correlation function reflects the OW at the momentum $\vec{k}=0$ as

$$S^{ll'}(\omega)=4N\sum_{\alpha=1}^{N}g^l_\alpha g^{l'}_\alpha\delta\left\{\omega-E_\alpha(0)\right\}. \tag{30}$$

In Fig. 4, the Raman spectra by OW in the (S-C/O-G) phase for LaVO$_3$, and in the (S-G/O-C) phase for YVO$_3$ (the low temperature phase) are presented. The two-orbiton scattering processes are considered. In spite of this processes, a sharp peak structure appears at the lower edge of the continuum. This is attributed to the one-dimensional character of the OW and the factor $h^l_{\alpha\beta}(\vec{k})$ in Eq. (28) which enhances the lower edge. As for the selection rule, the Raman scattering is only active for the (zz) polarization where both the incident and scattered light polarizations, $\vec{e}_{\vec{k}_i\lambda_i}$ and $\vec{e}_{\vec{k}_f\lambda_f}$, are parallel to the z axis. Through the interaction with the z-polarized lights, two electrons are exchanged between the d_{yz} (d_{zx}) orbitals in the NN sites along the z axis. We mention that the local modes discussed in the previous section, i.e. the $d_{xy}\to d_{yz}$ and $d_{xy}\to d_{zx}$ excitations, are not detected by the Raman scattering, since the exchange processes do not occur between the d_{xy} and d_{yz} (d_{zx}) orbitals. In Fig. 5, we show the Raman spectra

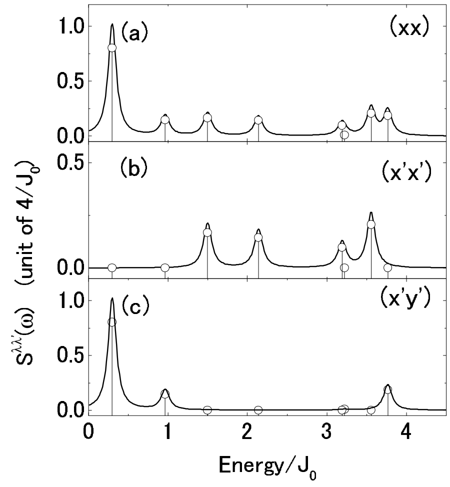

FIG. 5. Raman spectra for the $(d_{y(x+z)}/d_{y(x-z)}/d_{x(y+z)}/d_{x(y-z)})$-type OO state with FM order for YTiO$_3$. The one-orbiton scattering is considered. Symbols with vertical lines are the spectral weights of the delta-function. Continuous lines indicate $S^{\lambda_i\lambda_f}(\omega)$ where the delta-functions are replaced by the Lorentz functions and the width of the function is chosen to be $0.25J_0$. The polarizations of the incident and scattered photons are denoted as (λ, λ'). Other parameter values are the same as those in Fig. 2.

from OW in the $(d_{y(x+z)}/d_{y(x-z)}/d_{x(y+z)}/d_{x(y-z)})$-type OO. The one-orbiton scattering is considered in the calculation. The spectra being active for the (xx) and $(x'x')$ polarizations are the A_{1g} modes, and those for the (xx) and $(x'y')$ ones are the B_{1g} ones. Here, the x, y and z directions are chosen to be parallel to the TM-O bonds, and $x' = \frac{1}{\sqrt{2}}(x+y)$ and $y' = \frac{1}{\sqrt{2}}(-x+y)$. It is worth noting that all modes are inactive for the (zz) polarization in contrast to the case of vanadates. This originates from a cancellation from the one-orbiton scattering contributions from site i and its NN site $i+\delta_z$ along the z direction where the occupied orbitals have the mirror symmetry in terms of the xy plane between the two.

B. inelastic neutron scattering

Although the Raman scattering is a possible probe to detect OW as shown in the previous section, its observation is limited to be the OW at zero momentum in the one-orbiton scattering, and the joint density of states of OW in the two-orbiton scattering. In the t_{2g} OO systems of our present interest, it is possible to detect by the inelastic neutron scattering. Formulate the differential scattering cross section in the scattering of initial (scattered) neutron with momentum $\vec{k}_i(k_f)$, energy $\omega_i(\omega_f)$, and polarization $l_i(l_f)$ $(= x, y, z)$. The scattering cross section is given by

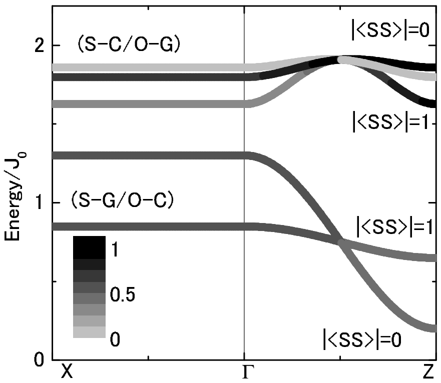

FIG. 6. Contour map of the scattering intensity $S^{zz}(\omega)$ in the inelastic neutron scattering in the (S-C/O-G) and (S-G/O-C)-phases for LaVO$_3$ and YVO$_3$ (the low temperature phase), respectively. The intensity is plotted as a unit of $2/J_0$. The spin polarizations of both the incident and scattered neutrons are chosen to be parallel to the z axis. The reciprocal vector is $\vec{G} = (000)$. Other parameter values are the same as those in Fig. 1.

$$\frac{d\sigma^2}{d\Omega d\omega_f} = \left(\frac{\gamma e^2}{m_N c^2}\right)^2 \left(\frac{1}{2} g F(\vec{K})\right)^2 \frac{k_f}{k_i} \times \sum_{l_i l_f} \left(\delta_{l_i l_f} - \kappa_{l_i}\kappa_{l_f}\right) S^{l_i l_f}(\vec{K}, \omega), \tag{31}$$

with $\vec{K} = \vec{k}_i - \vec{k}_f$, $\omega = \omega_i - \omega_f$, and $\vec{\kappa} = \vec{K}/|\vec{K}|$. $S^{l_i l_f}(\vec{K}, \omega)$ is the Fourier transform of the dynamical correlation function for the angular momentum operators L^l_{id} defined by

$$\begin{aligned} S^{l_i l_f}(\vec{r}_{id} - \vec{r}_{i'd'}, t) &= \langle L^{l_i}_{id}(t) L^{l_f}_{i'd'}(0)\rangle, \\ &= 2\langle O_{idT_1 l_i}(t) O_{i'd'T_1 l_f}(0)\rangle, \end{aligned} \tag{32}$$

where $\vec{r}_{id}$ is the position of the d-th TM ion in the i-the unit cell. In the linear spin wave approximation, $S(\vec{K}, \omega)$ is obtained as

$$S^{l_i l_f}(\vec{K}, \omega) = 2N \sum_{dd'} \sum_{\alpha=1}^{N} \delta\left\{\omega - E_\alpha(\vec{K})\right\} \times D^{l_i *}_{d\alpha} D^{l_f}_{d'\alpha} e^{i\vec{G}\cdot\vec{\delta}_{dd'}}, \tag{33}$$

where $D^l_{d\alpha}$ is defined by the Fourier transform of the angular momentum operator

$$O_{dT_1 l}(\vec{k}) = \sum_\alpha D^l_{d\alpha}(\vec{k}) \widetilde{\psi}_\alpha(\vec{k}). \tag{34}$$

$\vec{\delta}_{dd'}$ is a vector connecting the d- and d'-th TM ions in the same cell, and $\vec{G}$ is the reciprocal lattice vector. In contrast to the Raman scattering, the momentum dependence of the dispersion relation is detectable. The magnitude of the scattering intensity is expected to be the same order with that for the magnetic neutron scattering in magnets with $L = 1$.

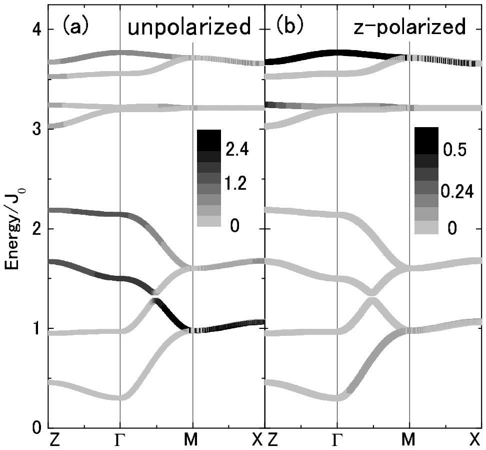

FIG. 7. Contour map of the inelastic neutron scattering spectra $S^{ll'}(\omega)$ for the $(d_{y(x+z)}/d_{y(x-z)}/d_{x(y+z)}/d_{x(y-z)})$-type OO state with FM order for YTiO$_3$. The intensity is plotted as a unit of $2/J_0$. The spin polarizations of the incident and scattered neutrons are chosen to be (a) unpolarized, and (b) parallel to the z axis. The reciprocal vector is $\vec{G} = (000)$. Other parameter values are the same with those in Fig. 2.

We present the scattering intensities of the inelastic neutron scattering in the (S-C/O-G) and (S-G/O-C)-phases (Fig. 6), and those in the FM order with the $(d_{y(x+z)}/d_{y(x-z)}/d_{x(y+z)}/d_{x(y-z)})$-type OO (Fig. 7). It is noted that the dispersive OW modes in vanadates are only detected by the z polarized neutron; the angular momentum L_z induces the excitations between the d_{yz} and d_{zx} orbitals. The local modes discussed in the previous section are active for the x and y polarized neutrons (not shown in Fig. 6). Therefore, the modes of OW are identified by utilizing the polarized neutron scattering. This is also seen in the contour map of the scattering intensity in YTiO$_3$; the scattering intensity for the OW modes in the higher energy bands are remarkable in the z-polarized neutrons. This implies that these modes mainly consist of the excitations between the d_{zx} and d_{yz} orbitals as explained in Sec. III.

V. SUMMARY AND DISCUSSION

In this paper, a theory of OW in perovskite titanates and vanadates with the triply degenerate t_{2g} orbitals is present. We examine the dispersion relations of OW in the (S-C/O-G)- and (S-G/O-C) phases for LaVO$_3$ and YVO$_3$ (the low temperature phase), respectively and that in the $(d_{y(x+z)}/d_{y(x-z)}/d_{x(y+z)}/d_{x(y-z)})$-type OO for YTiO$_3$. We demonstrated that characteristics of OW in these systems can be detected by utilizing the Raman and inelastic neutron scatterings.

In comparison with the OW in the manganites where the e_g orbital is ordered, both the excitation spectra and the observation methods are distinct qualitatively in the present t_{2g} orbital system. In particular, this is remarkably seen in vanadates where the so-called pure orbitals are ordered. Thus, the selection rules for the Raman and neutron scatterings are strict. For example, the two-orbiton scatterings with the z polarized photons dominate the Raman spectra. This is attributed to the orthogonality of the electron transfer integral between the NN vanadium sites. In the actual vanadates, there is the GdFeO$_3$-type lattice distortion which may make the one-orbiton scatterings possible. In the recent Raman scattering experiments in RVO$_3$, a new peak appears around 60meV in the (S-C/O-G) phase.[40] It is confirmed that this peak is active in the (zz) polarization configuration. We expect that this peak originates from OW excited by the two-orbiton scattering processes as discussed in Sec. III (Fig. 4).

In the case of YTiO$_3$, the dispersion relation of OW and the Raman and neutron scattering spectra are more complicated than those in vanadates. This is because of the mixed OO state with the four different orbitals in a unit cell. The present results are also distinct from those proposed in Ref. 18; the orbital excitations are examined in the OO states with high symmetry being different from the $(d_{y(x+z)}/d_{y(x-z)}/d_{x(y+z)}/d_{x(y-z)})$-type OO and incompatible with the crystal symmetry of YTiO$_3$. In the present results, as shown in Fig. 2, it is found, in contrast to the previous results,[18] that there are the anisotropy of the dispersion relations in the xy plane and along the z axis, the two kind groups of the OW with higher and lower energies appear, and the flat bands are not seen along the $(\pi\pi\pi)$-$(\pi\pi 0)$ direction. Actually, the inelastic neutron scattering experiments have started in YTiO$_3$.[41,17] The detailed comparison between the theoretical calculations and the experimental data can reveal nature of OW as well as that of OO in the t_{2g} orbital systems.

ACKNOWLEDGMENTS

Author would like to thank S. Maekawa, N. Nagaosa, G. Khaliullin, T. Hatakeyama, and S. Okamoto for their valuable discussions, and also thank Y. Tokura, S. Miyasaka, S. Shamoto, and S. Sugai for providing unpublished experimental data. This work was supported by KAKENHI from MEXT, and KURATA foundation. Part of the numerical calculation has been performed by the supercomputing facilities in IMR, Tohoku University.

---

[1] See, for a review, M. Imada, A. Fujimori, and Y. Tokura, Rev. Mod. Phys. **70**, 1039 (1998).
[2] Y. Tokura and N. Nagaosa, Science **288**, 462 (2000).

[3] M. Cyrot, and C. Lyon-Caen, Jour. Physique **36**, 253 (1975).

[4] A. G. Komarov, and L. I. Korovin, and E. K. Kudinov, Sov. Phys. Solid State **17**, 1531 (1975).

[5] S. Ishihara, J. Inoue, and S. Maekawa, Phys. Rev. B **55**, 8280 (1997).

[6] E. Saitoh, S. Okamoto, K. T. Takahashi, K. Tobe, K. Yamamoto, T. Kimura, S. Ishihara, S. Maekawa, and Y. Tokura, Nature **410**, 180 (2001).

[7] M. Gruninger, R. Ruckamp, M. Windt, P. Reutler, C. Zobel, T. Lorenz, A. Freimuth, and A. Revcolevshi, Nature **418**, 39 (2002).

[8] E. Saitoh, S. Okamoto, K. Tobe, K. Yamamoto, T. Kimura, S. Ishihara, S. Maekawa, and Y. Tokura, Nature **418**, 40 (2002).

[9] H. Nakao, Y. Wakabayashi, T. Kiyama, Y. Murakami, M. v. Zimmermann, J. P. Hill, D. Gibbs, S. Ishihara, Y. Taguchi, and Y. Tokura, Phys. Rev. B **66**, 184419 (2002).

[10] M. Itoh, M. Tsuchiya, H. Tanaka, and K. Motoya, Jour. Phys. Soc. Jpn. **68**, 2783 (1999).

[11] H. Ichikawa, J. Akimitsu, M. Nishi, and K. Kakurai, Physica B **281&282**, 482 (2000).

[12] D. A. MacLean, H.-N. Ng, and J. E. Greedan, Jour. Sol. Stat. Chem. **30**, 35 (1979).

[13] S. Ishihara, T. Hayakeyama, and S. Maekawa, Phys. Rev. B **65**, 064442 (2002).

[14] T. Mizokawa, and A. Fujimori, Phys. Rev. B **54**, 5368 (1996), and T. Mizokawa, D. I. Khomskii, and G. A. Sawatzky, Phys. Rev. B **60**, 7309 (1999).

[15] H. Sawada, N. Hamada, K. Terakura, and T. Asada, Phys. Rev. B **53**, 12742 (1996), and H. Sawada, and K. Terakura, Phys. Rev. B **58**, 6831 (1998).

[16] M. Mochizuki, and M. Imada, Jour. Phys. Soc. Jpn. **69**, 1982 (2000), ibid **70**, 1777 (2001).

[17] C. Ulrich, G. Khaliullin, S. Okamoto, M. Reehuis, A. Ivanov, H. He, Y. Taguchi, Y. Tokura, and B. Keimer, Phys. Rev. Lett. **89**, 167202 (2002).

[18] G. Khaliullin, and S. Okamoto, Phys. Rev. Lett. **89**, 167201 (2002).

[19] Y. Ren, T. T. M. Palstra, D. I. Khomskii, E. Pellegrin, A. A. Nugroho, A. A. Menovski, and G. A. Sawatzky, Nature, **396**, 441 (1998).

[20] S. Miyasaka, Y. Okimoto, and Y. Tokura, Jour. Phys. Soc. Jpn. **71**, 2086 (2002).

[21] S. Miyasaka, Y. Okimoti, M. Iwama, and Y. Tokura, Phys. Rev. B **68**, 100406 (2003).

[22] P. Bordet, C. Chaillout, M. Marezio, Q. Huang, A. Santro, S. -W. Cheong, H. Takagi, C. S. Oglesby, and B. Batlogg, Jour. Sol. Stat. Chem. **106**, 253 (1993).

[23] H. Kawano, H. Yoshizawa, and Y. Ueda, Jour. Phys. Soc. Jpn. **63**, 2857 (1994).

[24] M. Noguchi, A. Nakazawa, S. Oka, T. Arima, Y. Wakabayashi, H. Nakao, and Y. Murakami, Phys. Rev. B **62**, R9271 (2000).

[25] G. R. Blake, T. T. M. Palstra, Y. Ren, A. A. Nugroho, and A. A. Menovsky, Phys. Rev. Lett. **87**, 245501 (2001).

[26] C. Ulrich, G. Khaliullin, J. Sirker, M. Reehuis, M. Ohl, S. Miyasaka, Y. Tokura, and B. Keimer, (unpublished) cond-mat/0211589.

[27] G. Khaliullin, P. Horsch, and A. M. Olés, Phys. Rev. Lett. **86**, 3879 (2001), and J. Sirker, and G. Khaliullin, Phys. Rev. B **67**, 100408 (2003).

[28] Y. Motome, H. Seo, Z. Fang, and N. Nagaosa, Phys. Rev. Lett. **90**, 146602 (2003).

[29] Z. Fang, N. Nagaosa, and K. Terakura, Phys. Rev. B **67**, 035101 (2003).

[30] T. H. De Silva, A. Joshi, M. Ma, and F. C. Zhang, (unpublished) cond-mat/03024989.

[31] M. Gell-Mann, and Y. Ne'eman. *The eightfold way*, (Benjamin, New York, 1964).

[32] K. I. Kugel, and D. I. Khomskii, Sov. Phys. Solid, State, **17**, 285 (1975).

[33] K. Kikoin, O. Entin-Wohlman, V. Fleurov, and A. Aharony, Phys. Rev. B **67**, 214418 (2003).

[34] M. Itoh, H. Adachi, H. Nakao, Y. Murakami, Y. Taguchi, Y. Tokura, K. Kato, E. Nishibori, M. Takata, M. Sakata, H. Miyagawa, S. Nanao, H. Maruyama, E. Arawaka, and K. Namikawa, Meeting Abstract of the Physicsl Society of Japan, 2001 Autumn Meeting, **56**, Part 3, 341 (2001).

[35] D. Janssen, R. V. Jolos, and F. Donau, Nucl. Phys. A **224**, 93 (1974).

[36] A. Klein, and E. R. Marshalek, Rev. Mod. Phys. **63**, 375 (1991).

[37] J. Inoue, S. Okamoto, S. Ishihara, W. Koshibae, Y. Kawamura, and S. Maekawa, Physica B **237-238**, 51 (1997).

[38] S. Okamoto, S. Ishihara, and S. Maekawa, Phys. Rev. B **66**, 104435 (2001).

[39] P. B. Allen, and V. Pereveinos, Phys. Rev. Lett. **83**, 4828 (1999), and V. Pereveinos, and P. B. Allen, Phys. Rev. B **64**, 085118 (2001).

[40] S. Miyasaka and Y. Tokura (unpublished).

[41] S. Shamoto, F. Iga, M. Tsubota, T. Kajitani, ISIS Experimental Report, RB Num.13662, Date of Report 03/03/03, MARI.